# Parametric Modeling of Microwave Structure with Customization Responses by Combining RBF Neural Network and Pole-Residue-Based Transfer Functions

*Yuhong MA, Shuang WU, Ye YUAN, Naichang YUAN*

State Key Laboratory of Complex Electromagnetic Environment Effects on Electronics and Information System, National University of Defense Technology, Deya Road 109, 410073 Changsha, China

1160668326@qq.com, ws02114006@163.com, 767411434@qq.com, yuannaichang@hotmail.com

Submitted August 14, 2021 / Accepted April 5, 2022

**Abstract.** *This paper proposed a parametric modeling technique for the microwave structures with a customization magnitude response by combining the RBF neural network and pole-residue-based transfer functions. The Latin hypercube sampling method is used for sampling given physical ranges and obtaining the EM behaviors of the microwave structures. A pole sorting process and a modified pole-residues splitting process are proposed to solve the pole sequence chaos and order-changing problems which occur in the modeling process. The pole-residues parameters after the above preprocessing steps are used as the inputs of the RBF neural network and the physical parameters are used as the outputs of RBF network. Then, the known magnitude response of the microwave structure are used as the prior knowledge to guide obtaining the goal pole-residues values corresponding to the giving magnitude response specification. After the training process of the RBF model, the goal pole-residues are input into the trained RBF network and the goal physical parameters corresponding to the customization responses is obtained. Finally, this model technique is illustrated by the two examples of microwave structures.*

## Keywords

Parametric modeling, customization response, RBF neural network, pole-residue-based transfer functions

## 1. Introduction

The EM simulation is time-consuming and computationally expensive in the parameter sweep and tuning steps. Parametric modeling of microwave components has been a research hotspot to accelerate the design and tuning process of microwave components and some progress had been made in [1], [2]. In the parametric modeling of microwave components, artificial neural networks (ANNs) working as the useful tools in EM parametric modeling and design optimization has been researched in [3–9].

The popular idea of parametric modeling of microwave components is using the transfer function to fit the EM responses under different geometrical variations. The coefficients of the transfer function(TF) change as the geometrical variations change, and ANN is used to learn the non-linear relationship between the transfer function coefficients and the geometrical parameters. Some key technical challenges in this model process have been researched recently. In [10], rational format of the transfer function proposes the sensitivity-analysis-based neuro-TF model is used. Compared with the original rational format neuro-TF model, the model proposed in [10] achieves a high fitting accuracy with less training samples. In [11], the EM responses are classified into several categories based on the TF orders, and the data classification technology SVM (support vector machine) is used to classify geometric variables and solve the problem that the order of transfer function is not uniform. Reference [12] analyses the advantages of using pole-residue-based transfer functions compared with using the rational transfer function. Besides, reference [12] proposes a novel pole-residue tracking technique to solve the coefficient discontinuity due to the transfer function order changing and the EM examples simulation results prove the effective of this pole-residue tracking technique. Based on the [12], reference [13] proposed a pole-residue-based electromagnetic (EM) sensitivity analysis neuro-transfer function technique which performs well in the limited training data. Recently, based on the model-order reduction (MOR) technique, reference [14] proposed a novel poles matching technique through Pade via lanczos and EM sensitivities, and the simulated application examples proves that this technique could perform well in the large geometrical variations.

The mainstream way in the above EM behavior parametric modeling technique is that the ANN is the open model with the geometrical parameters as the model input and the coefficients as the model output.

In this paper, the pole-residues parameters are used as the input of the RBF neural network and the physical parameters are used as the output of the RBF neural network.

DOI: 10.13164/re.2022.0185

The equivalent circuit or the known magnitude response of the microwave structure are used as the prior knowledge to guide obtaining the goal pole-residues values. The goal pole-residues is input into the trained RBF network and we can get the goal physical parameters directly. Finally, the microwave components are used as the examples to prove the feasibility of the proposed technique.

## 2. Proposed Customization Parametric Model

We present the parametric modeling technique in [12] firstly before introducing our technique. For the given physical parameters ranges, a set of EM responses corresponding to the different physical parameters are obtained by using simulation software. Then, the following transfer function (1) is used to fit the above EM responses by using the vector fitting technique proposed in [15].

$$H(p,r,w) = \sum_{i=1}^{N_k} \left( \frac{r_i}{\mathrm{j}w - p_i} + \frac{r_i^*}{\mathrm{j}w - p_i^*} \right) \tag{1}$$

Since each complex pole ($p$) or residue ($r$) has a conjugate, the poles which has negative imaginary part and its corresponding residues are removed. The major idea of modeling the EM behavior in [12] is using neural networks to learn the relationship between the physical parameters and each pair of pole and residue value. The physical parameters are used as the input of the neural network and the pole-residues are used as the output of the neural network. This modeling method expresses that different pairs of poles and residues are mutually independent and ignores the relationship between the poles and residues. Actually, this mutually relationship between the transfer function parameters (poles and residues) could has a significant effect on the EM responses.

To give a more explicit picture, the 3D frequency selective surface (FSS) shown in Fig. 1 is used as the test subject to explain the mutual effect between the poles and residues. As a kind of spatial filter and secondary radiant antenna, the FSS not only has the performance of the filter but also has some characteristics of the antenna. The origin simulating frequency range of the test object is 0.5 GHz–7.5 GHz. According to the [12], frequency scaling and shifting method is an effective way to transfer the real poles into complex poles, so the origin frequency range is scaled and shifted to 0.9 GHz–1.1 GHz. After the above frequency scaling and shifting process, we use the vector fitting technique to process the EM behavior and obtain the pole-residue values.

Six random parameter sets listed in Tab. 1 are used as the testing physical parameter sets. The poles and residues values of the EM behavior corresponding to these six parameter sets are obtained by using the vector fitting technique. Then, a random error with the value of 0.1% is added to the poles and residues values. For the six test geometrical samples, the magnitude responses of the pole-residue-based model after introducing the random error and its corresponding origin EM responses are shown in Fig. 2.

Although the random errors of the pole-residues only has 0.1%, this infinitesimal disturbance destroys the mutually relationship between the poles and residues as shown in Fig. 2. In this paper, considering this mutual relationship between the poles and residues, we propose a customization parametric modeling based on the transfer function and the RBF neural network. The detail process of the proposed model is discussed in the following subsection.

| Sample | $l_1$ | $l_2$ | $l_3$ | $w_1$ | $w_2$ | $w_3$ | $s$ |
|---|---|---|---|---|---|---|---|
| **1** | 12.53 | 10.22 | 13.37 | 4.12 | 0.095 | 0.82 | 0.22 |
| **2** | 11.15 | 9.44 | 13.01 | 3.11 | 0.129 | 1.267 | 0.145 |
| **3** | 11.85 | 9.68 | 14.82 | 3.23 | 0.116 | 0.766 | 0.23 |
| **4** | 12.58 | 9.95 | 14.67 | 3.00 | 0.123 | 0.936 | 0.116 |
| **5** | 12.17 | 9.35 | 14.89 | 3.80 | 0.207 | 0.958 | 0.274 |
| **6** | 12.50 | 10.66 | 14.56 | 3.49 | 0.22 | 1.38 | 0.101 |

**Tab. 1.** Geometrical parameter sets of the testing object (unit: mm).

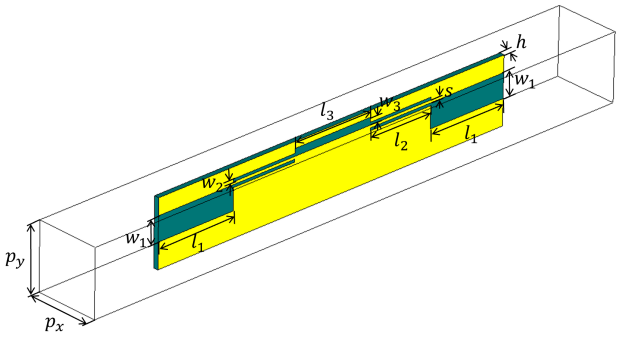


**Fig. 1.** Structure of the 3D FSS. The seven geometrical parameters of the structure are [$l_1$, $l_2$, $l_3$, $w_1$, $w_2$, $w_3$, $s$], with $p_x = p_y = 10$ mm, $h = 0.762$ mm, substrate: FR-4.

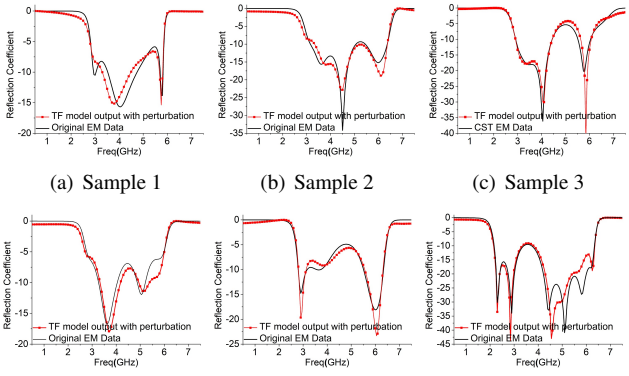


(a) Sample 1 (b) Sample 2 (c) Sample 3

(d) Sample 4 (e) Sample 5 (f) Sample 6

**Fig. 2.** The original EM behavior of the test object and its corresponding pole-residue-based model output after introducing the random error.

## 2.1 Sorting Process

In the proposed method, the Latin hypercube sampling method is used to sample the physical parameters. Using the Latin hypercube sampling method results in the imaginary of different pole for microwave component has approximate imaginary part, and the pole-sorting way in [12] based on the value of the pole imaginary part may loses its effectiveness. The pole distribution pattern of the 3D FSS is used to explain this phenomenon. 175 sets of physical parameters used to simulate EM behavior are generated randomly within the range listed in Tab. 3. The orders $N_{\mathrm{k}}$ of the transfer function for the simulated EM behaviors are from 8 to 9. The samples size of $N_{\mathrm{k}} = 8$ is 90, and the samples size of $N_{\mathrm{k}} = 9$ is 85. The poles distribution under different order $N_{\mathrm{k}}$ are shown in Fig. 3. We take poles distribution pattern for $N_{\mathrm{k}} = 9$ as an example to explain this chaos of poles sequence. The approximate distributions for each pole are marked in Fig. 3. According to Fig. 3, the sequences of the imaginary parts in P2 and P9, P6 and P7 occur chaos. In order to align the order of poles, a new pole-sorting way is proposed.

The proposed pole-sorting way is similar to the K-means clustering method. The pole-residues samples with the effective order $N_{\max}$ are sorted firstly. For the samples with the effective order $N_{\max}$, the sample closest to the center geometrical point of the Latin hypercube sampling range is defined as $x_0$. The poles sequence of the $x_0$ is sorted in an ascending sequence according to the values of their complex modulus value parts firstly, while the sequence of residues are sorted with their corresponding poles. Assuming the flatten pole matrix of the sample $x_0$ is

$$\mathbf{F}_{x_0} = \left[p_{\mathrm{r1}}^{x_0}, p_{\mathrm{i1}}^{x_0}; \cdots; p_{\mathrm{r}n}^{x_0}, p_{\mathrm{i}n}^{x_0}; \cdots; p_{\mathrm{r}N_{\max}}^{x_0}, p_{\mathrm{i}N_{\max}}^{x_0}\right] \tag{2}$$

where $n$ is the index of the poles, $p_{\mathrm{r}n}^{x_0}$ is the real part of the $n$th pole in $x_0$ and $p_{\mathrm{i}n}^{0}$ the imaginary part of the $n$th pole in $x_0$. The flatten pole matrix of the $x_0$ is defined as the center of clustering and this cluster center contains $N_{\max}$ poles.

The sample $x_1$ is any one of the samples with the effective order of $N_{\max}$. The out-of-order flatten poles matrix of $x_1$ is $\mathbf{F}_{x_1} = [p_{\mathrm{r1}}^{x_1}, p_{\mathrm{i1}}^{x_1}; \cdots; p_{\mathrm{r}N_1}^{x_1}, p_{\mathrm{i}N_1}^{x_1}]$. We take out the parameter data of the $m$th pole from $\mathbf{F}_1$, i.e., $\mathbf{F}_1(m,:) = [p_{\mathrm{r}m}^{x_1}, p_{\mathrm{i}m}^{x_1}]$. The next step is to find this $m$th pole corresponds to which pole in the center of clustering. The indicator to measure the difference between the two poles is defined as:

$$G_m(n) = ||(\mathbf{F}_{x_0}(n,:) - \mathbf{F}_{x_1}(m,:))||_2 \tag{3}$$

where $\mathbf{F}_{x_0}(n,:)$ is the parameter of $n$th pole in $x_0$. The correct index of the $m$th pole in the sample $x_1$ is $M = \arg \min_{n \in 1,2,\cdots,N_{\max}} G_m(n)$. The above process is performed iteratively for $N_{\max}$ times until the indexes of $N$ poles in sample $x_1$ are determined. In the above sorting process, two poles of the sample $x_1$ may been divided into a same index, as shown in Fig. 4. In the samples with same order,

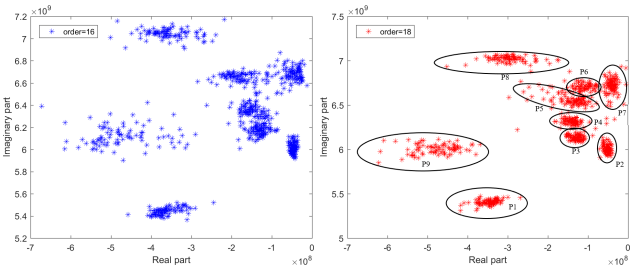


(a) $N_{\mathrm{k}} = 8$ (b) $N_{\mathrm{k}} = 9$

**Fig. 3.** The poles distribution patterns.

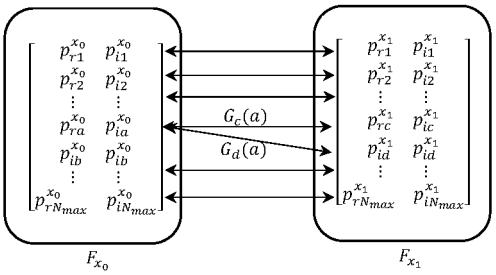


**Fig. 4.** Disorder phenomenon in pole sorting process.

the correct pole correspondence between samples is one-to-one. In this case, the $b$th pole in sample $x_0$ misses the corresponding pole in $\mathbf{F}_{x_0}$, and $a$th pole in $\mathbf{F}_{x_0}$ has two corresponding pole in $\mathbf{F}_{x_1}$. In this situation, the smaller one of the $G_c(a)$ and $G_c(b)$ is assigned to the index $p_a^{x_0}$ and the other pole is assigned to the pole $p_b^{x_0}$. After the above pole sequence sorting process, the residues sequence is sorted with their corresponding poles. The sample $x_2$ is another samples with the effective order $N_{\max}$ and the pole-residue sequence of the sample $x_2$ is sorted through above steps similarly. The pole sequence of the samples with the effective order $N_{\max} - 1$ are sorted similarly.

## 2.2 Modified Pole-Residues Splitting Process

Reference [12] proposes that the order-changing phenomenon is caused by that a new pole splitting from the one of the primary poles for the geometrical parameters changing. Detail discussion of this pole splitting phenomenon is discussed in [12]. To prevent repetition, it is not described in this paper. In [12], a novel pole-residue tracking technique for order-changing problem in the case of DOE sampling method is proposed. The Pole-Residue distribution pattern of the Latin hypercube sampling method is different with the one of the DOE sampling method. Based on the Pole-Residue splitting technique in the [12], a modified Pole-Residue splitting technique for the Latin hypercube sampling method is proposed in this paper.

We split the samples with $N_{\mathrm{k}} = N_{\min}$ firstly. Let us pick a sample ($x_{\mathrm{k}}$) from $N_{\mathrm{k}} = N_{\min}$ randomly. This sample has two parameters including physical parameters and pole parameters ($F_{\mathrm{k}}$). Slight changes in physical parameters between samples lead to slight changes in pole parameters, and

we use this relationship to confirm which pole of $x_{\mathrm{k}}$ should be selected to be spilt. From the samples with effective order of $N_{\min}+1$, we can easily find the sample $x_{\mathrm{L}}$ which has the minimum Euclidean distance of physical parameter to $x_{\mathrm{k}}$. We split the poles of the $x_{\mathrm{k}}$ separately, and $N_{\min}$ times of trials are performed. In the $m$th trial, the $m$th pole of the $x_{\mathrm{k}}$ is select to be split and the flatten pole matrix of sample $x_{\mathrm{k}}$ after split process is

$$\mathbf{F}_{x_{\mathrm{k}}}=\begin{bmatrix} p_{\mathrm{r}1}^{x_{\mathrm{k}}} & p_{\mathrm{i}1}^{x_{\mathrm{k}}} \\ \vdots & \\ p_{\mathrm{r}m}^{x_{\mathrm{k}}} & p_{\mathrm{i}m}^{x_{\mathrm{k}}} \\ p_{\mathrm{r}m}^{x_{\mathrm{k}}} & p_{\mathrm{i}m}^{x_{\mathrm{k}}} \\ \vdots & \\ p_{\mathrm{r}N_{\min}}^{x_{\mathrm{k}}} & p_{\mathrm{i}N_{\min}}^{x_{\mathrm{k}}} \end{bmatrix}. \tag{4}$$

The flatten poles matrix of sample $x_{\mathrm{L}}$ is

$$\mathbf{F}_{x_{\mathrm{L}}}=\begin{bmatrix} p_{\mathrm{r}1}^{x_{\mathrm{L}}} & p_{\mathrm{i}1}^{x_{\mathrm{L}}} \\ \vdots & \\ p_{\mathrm{r}(N_{\min}+1)}^{x_{\mathrm{L}}} & p_{\mathrm{i}(N_{\min}+1)}^{x_{\mathrm{L}}} \end{bmatrix}. \tag{5}$$

The expression to measure the pole-residue difference between the sample $x_{\mathrm{k}}$ and sample $x_{\mathrm{L}}$ is defined as follows:

$$D_m=\sum_{i=1,j=1}^{N_{\min}+1,2}\left(\mathbf{F}_{x_{\mathrm{k}}}-\mathbf{F}_{x_{\mathrm{L}}}\right)_{i,j}^2. \tag{6}$$

The above process is performed for $N_{\min}$ times. According to the [12], the poles and residue should keep continuous for the slight variation of the geometrical parameters changing and the correct pole splitting way should result in the minimum pole-residue difference. Therefore, the $M$th pole corresponding to the minimum value of $D_m$ is used to be the splitting pole, and

$$M=\arg\min_{m=1,\cdots,N_{\min}}(D_m). \tag{7}$$

After finishing this process of all the samples with $N=N_{\min}$ , the minimum order of the entire samples increases to $N_{\min}+1$. The pole-residue splitting process performs iteratively until the minimum effective order is equal to the maximum effective order $N_{\max}$. All the samples would have the same orders $N_{\max}$ after the above process.

## 2.3 RBF Neural Network Training Process

After above process, the neural network model to learn the relationship between the poles-residues vector and the physical parameters is discussed in this section. Before constructing the neural network to fit this relationship, let us discuss how to obtain the goal pole-residues parameters corresponding to the customization response.

For the microwave structure with the known equivalent circuit model or norm magnitude response liking the generalized Chebyshev equal-ripple response, the goal magnitude response can been obtained through the equivalent circuit simulation or normal magnitude response equation. Based on the goal magnitude response, the simulate anneal (SA) optimization algorithm is used to obtain the pole-residues values corresponding to the goal magnitude response. We first transform the original simulated pole-residues data after the above pole sorting and splitting process into a vector and the flatten poles-residues vector is:

$$\begin{aligned}\mathbf{T}^k=\Big[&p_{\mathrm{r}1}^k,p_{\mathrm{i}1}^k,\cdots,p_{\mathrm{r}N_{\max}}^k,p_{\mathrm{i}N_{\max}}^k,\\ &r_{r1}^k,r_{i1}^k,\cdots,r_{rN_{\max}}^k,r_{iN_{\max}}^k\Big]\end{aligned} \tag{8}$$

where $k$ is the index of the samples. These flatten vectors are chosen as the start pole-residues parameters of the SA optimize process to obtain the goal pole-residues parameters, and the loss function is defined as:

$$\begin{aligned}&[p_{\mathrm{goal}},r_{\mathrm{goal}}]=\arg\min\sum_{w_{\min}}^{w_{\max}}\left(\mathrm{abs}(H(p,r,w)-S_{\mathrm{goal}}(w))\right)^2,\\ &H(p,r,w)=\sum_{1}^{2*N_{\max}}\frac{r_i}{\mathrm{j}w-p_{\mathrm{i}}}\end{aligned} \tag{9}$$

where $S_{\mathrm{goal}}$ is the goal magnitude response. After above processes, the goal pole-residues vector is obtained. Before using the processed pole-residue vector $\mathbf{T}^k$ as the neural network input, we notice that some poles of the samples are mixed. For example, the P5 and P6 shown in Fig. 3 splits from a same pole. After the pole splitting process, the distributions of the P5 and P6 have a same region. This region mixture of poles results in the difficulty to figure out the correct sequence of P5 and P6 in the goal pole-residue vector. To avoid this disorder phenomenon of goal pole-residues vector, the parameters of the mixture poles ($r^{\mathrm{mixture}}$, $p^{\mathrm{mixture}}$) and corresponding residues are transfer into the parameters in rational transfer function format through the following equation:

$$\frac{\sum_{i=1}^{N_{\mathrm{s}}}a_i(s)^i}{1+\sum_{i=1}^{2*N_{\mathrm{s}}}b_i(s)^i}=\sum_{1}^{N_{\mathrm{s}}}\frac{r_i^{\mathrm{mixture}}}{s-p_{\mathrm{i}}^{\mathrm{mixture}}} \tag{10}$$

where $s=\mathrm{j}w$ and $N_{\mathrm{s}}$ is the number of the mixture poles. The modified pole-residues vector of $k$th sample is

$$\begin{aligned}\mathbf{T}^k=\big[&p_{\mathrm{r}1}^k,p_{\mathrm{i}1}^k,r_{\mathrm{r}1}^k,r_{\mathrm{i}1}^k,\cdots,r_{\mathrm{r}N_{\max}-N_{\mathrm{s}}}^k,r_{\mathrm{i}N_{\max}-N_{\mathrm{s}}}^k,\\ &a_{\mathrm{r}1},a_{\mathrm{i}1},b_{\mathrm{r}1},b_{i1},\cdots,b_{\mathrm{r}N_{\mathrm{s}}},b_{\mathrm{i}N_{\mathrm{s}}}\big].\end{aligned} \tag{11}$$

Then, the RBF networks is used as the fitting tool with the goal pole-residues coefficients as the model input and the geometrical parameters as the model output.

The RBF networks use gaussian kernel function as the activation functions, while the BP networks use the sigmoid/ReLu/tanh function as the activation functions. Compared with the BP neutral network, the RBF network has fast convergence rate and the better generalization ability. Besides, Poggio and Girosi has proven that the RBF network is the best approximation of a continuous function.

The structure of the RBF neural network used in our paper is shown in Fig. 5. The $x$ is the input of the neural network and $y$ is the output of the neural network. $R_1, \cdots, R_{\mathrm{h}}$ represents the hidden layers. The activation function we used is the Gaussian function.

The input of the RBF neutral network is the modified pole-residues vector $\mathbf{T}^k$ shown in (11) and the desire output of the RBF neutral network is the corresponding physical parameters. After the neural network training process, the goal pole-residue vector is input to the trained RBF neural network and the goal physical parameter is obtained.

The flowchart of the overall parametric model process of the microwave structure with customization magnitude response is shown in Fig. 6.

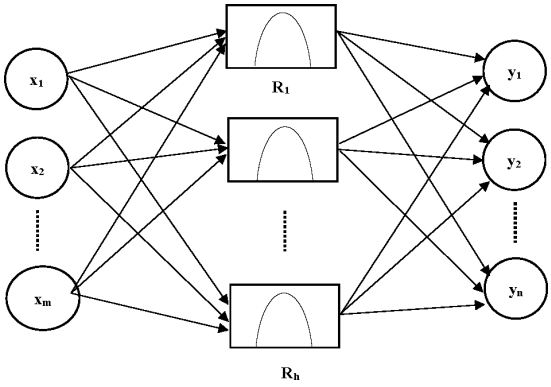


**Fig. 5.** The structure of the RBF neural network.

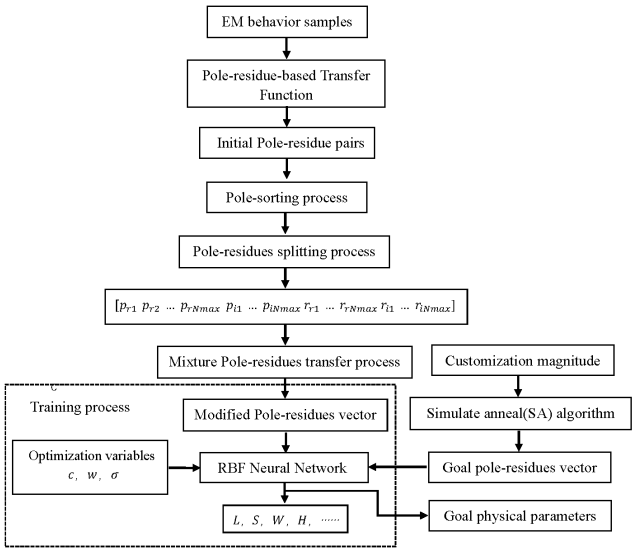


**Fig. 6.** The flowchart of the overall modeling process.

# 3. Experimental Verification Examples

## 3.1 Customization Modeling of a Three-Pole H-plane Filter

The waveguide filter shown in Fig. 7 with a third-order Chebyshev response is used as the example to validate the above modeling technique. The CST Studio Suite 2019 software is used to perform the full-wave simulation and generate the dataset for modeling process. The origin simulating frequency range of the test object is 11 GHz–14 GHz.

150 EM behavior samples are generated by using the Latin hypercube sampling method with the parameters ranges as defined in Tab. 2. The minimum orders $N_{\mathrm{k}}$ of transfer functions stay unchanged at order five for all samples. The above dataset is randomly divided into two parts: 80 samples as a training set and 70 samples as a test set. The node number of the hidden layer of the RBF is set as 30.

After the training process, the average error of the testing samples is 1.4%. The difference between the proposed model output and the true value of the test set is shown in Fig. 8. According to the Fig. 8, the output of our proposed model is consistent well with the actual data. Moreover, the DOE method is compared with the Latin hypercube sampling method here. The geometrical variable steps of the DOE method are listed in Tab. 2, and the samples obtained by the Latin hypercube sampling method is used as the test set. After the training process, the testing errors of the DOE method is 9.5%. Thus, the Latin hypercube sampling method is better than the DOE method for the proposed modeling method.

| **Geometrical variables** | | $a$ | $l_1$ | $l_2$ | $t$ | $w_1$ | $w_2$ |
|---|---|---|---|---|---|---|---|
| **Range** | **Min** | 17 | 12.5 | 13.5 | 1.5 | 8.5 | 5.15 |
| | **Max** | 21 | 14.5 | 16 | 2.5 | 9.5 | 6.15 |
| **DOE method step** | | 0.29 | 0.14 | 0.18 | 0.06 | 0.07 | 0.07 |

**Tab. 2.** Definition of training and testing data (unit: mm).

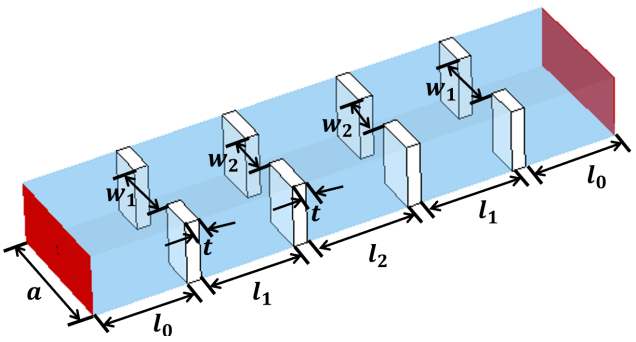


**Fig. 7.** Structure of the three-pole H-plane filter for EM simulation and parametric modeling. The six geometrical parameters of the filter are $x = [a, l_1, l_2, t, w_1, w_2]$, with $l_0 = 13.7$ mm.

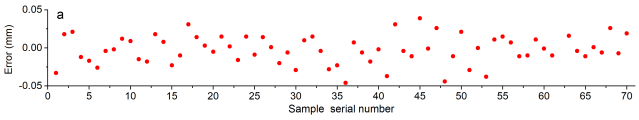


(a) Parameter $a$

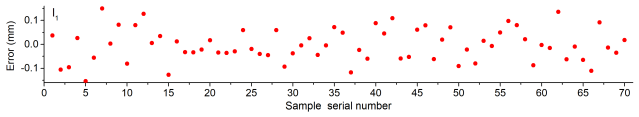


(b) Parameter $l_1$

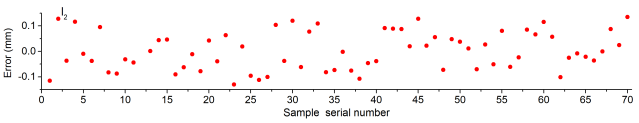


(c) Parameter $l_2$

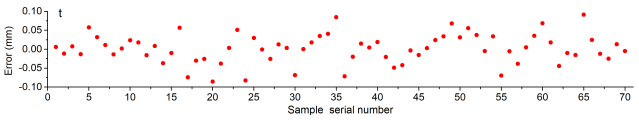


(d) Parameter $t$

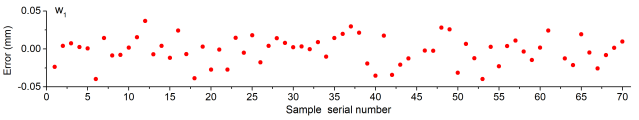


(e) Parameter $w_1$

**Fig. 8.** The comparison between the model output and the true value of the physical parameters.

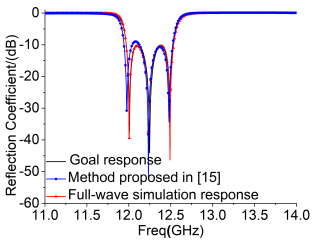


(a) Specification 1

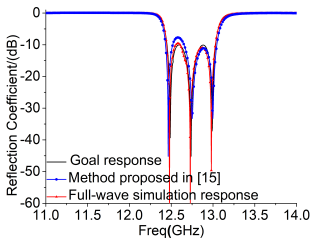


(b) Specification 2

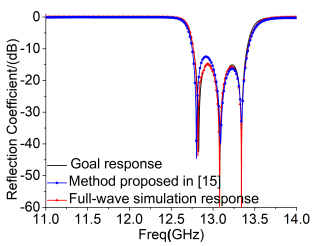


(c) Specification 3

**Fig. 9.** The calculated goal magnitude responses and the full-wave simulated response corresponding to the specifications.

Three norm Chebyshev magnitude responses shown in Fig. 9 are used as the testing dataset to validate the effectiveness of the customization modeling. The goal magnitude responses are obtained by the Filter Designer 3D kit in the CST software, and the specification settings of the three goal reflection coefficients are:

**Specification 1**:
$FreqRange$ = 11.97 GHz–12.53 GHz, $RL = -10$ dB;

**Specification 2**:
$FreqRange$ = 12.44 GHz–13.02 GHz, $RL = -10$ dB;

**Specification 3**:
$FreqRange$ = 12.79 GHz–13.39 GHz, $RL = -15$ dB;

where $RL$ represents return loss. The physical parameters obtained by the proposed model corresponding to the above specifications are

**Specification 1**: $a = 20.2764$, $l_1 = 12.754$, $l_2 = 14.0912$, $t = 1.4855$, $w_1 = 8.9672$, $w_2 = 6.034$;

**Specification 2**: $a = 17.897$, $l_1 = 12.832$, $l_2 = 14.1708$, $t = 1.6340$, $w_1 = 8.7945$, $w_2 = 6.086$;

**Specification 3**: $a = 17.1062$, $l_1 = 12.4069$, $l_2 = 13.5834$, $t = 1.6589$, $w_1 = 9.0992$, $w_2 = 6.483$.

By using the above physical parameter sets as the initial values, the tuning process is used to obtain accurate physical parameters corresponding to the goal magnitude specifications. After several minute tuning process, the exact physical parameters corresponding to the three goal magnitude specifications are

**Specification 1**: $a = 20.1932$, $l_1 = 12.896$, $l_2 = 13.9285$, $t = 1.4067$, $w_1 = 8.8956$, $w_2 = 6.1501$;

**Specification 2**: $a = 17.7603$, $l_1 = 12.9339$, $l_2 = 14.0273$, $t = 1.54426$, $w_1 = 8.69834$, $w_2 = 6.2$;

**Specification 3**: $a = 17.1344$, $l_1 = 12.2755$, $l_2 = 13.5$, $t = 1.5641$, $w_1 = 8.94045$, $w_2 = 6.38053$.

The full-wave simulation results corresponding to the above the three goal physical parameters are show in Fig. 9. The results of the model proposed in [12] are shown in Fig. 9 as well.

The model proposed in [12] is a forward model, and the parameters of pole-residues transfer function has the strong sensitivity for the geometrical variable changing [1]. Therefore, the robustness of the forward model is not good in parametric modeling of microwave structures. For our proposed model, the three physical parameters corresponding to the three specifications obtain by the proposed model are consistent well with the exact three physical parameters obtained by the full-wave simulation. Although the goal values of some parameters including $w_2$ and $t$ are out of the scope listed in Tab. 2, the parameters of the model output are basically nearby its exact physical parameters and this proves the proper generalization ability of our proposed parametric modeling technique.

### 3.2 Customization Modeling of the 3D Frequency Selective Surface

The 3D frequency selective surface (FSS) shown in Fig. 1 with wide geometrical ranges is used as the second example to validate the proposed parametrical modeling method. The equivalent circuit structure of the 3D FSS is shown in Fig. 10.

175 sets of physical parameters used to simulate EM behavior are generated randomly within the range listed in Tab. 3. Based on the EM behaviors, the pole-residues vector dataset is obtained by using the proposed model procedure. Then, the whole dataset is randomly divided into two parts: 85 samples as a training set and 65 samples as a test set. The node number of the hidden layer of the RBF is set as 35. After the training process, the average error of the testing samples is 4.8%.

Based on the equivalent circuit simulation, three goal magnitudes shown in Fig. 11 are obtained and used as the test objects. The specifications and the equivalent circuit parameters corresponding to the three goal magnitudes are listed in Tab. 4.

Based on the equivalent circuit magnitude response shown in Fig. 11(a), the physical parameters obtained by the proposed model are $l_1 = 12.5999$, $l_2 = 9.73254$, $l_3 = 14.2472$, $w_1 = 3.80239$, $w_2 = 0.286227$, $w_3 = 1.03839$, $s = 0.0791056$ and the full-wave simulation result corresponding to this physical parameters is shown in Fig. 11(a). As we can seen, the magnitude response corresponding to the model output physical parameters is basically consistent with the goal magnitude response as shown in Fig. 11(a). The proposed model can provide a reliable output in spite of giving a rough goal magnitude response.

The physical parameter sets corresponding to the two other goal magnitude response obtained by the proposed model are $l_1 = 12.0872$, $l_2 = 9.3691$, $l_3 = 13.6867$, $w_1 = 3.5817$, $w_2 = 0.2539$, $w_3 = 1.326$, $s = 0.1124$ and $l_1 = 13.8617$, $l_2 = 10.9856$, $l_3 = 15.6605$, $w_1 = 3.80047$, $w_2 = 0.392006$, $w_3 = 1.432$, $s = 0.060$ respectively. These two parameters sets are used as the initial points of the tuning process and the exact physical parameters corresponding to the Specification 2 and Specification 3 are obtained after the full-wave tuning process. After the above process, the exact physical parameters corresponding to the Specification 2 and Specification 3 are $l_1 = 12.01$, $l_2 = 9.30$, $l_3 = 13.988$, $w_1 = 3.749$, $w_2 = 0.2401$, $w_3 = 1.398$, $s = 0.1$ and $l_1 = 14.2$, $l_2 = 11.1174$, $l_3 = 15.8458$, $w_1 = 4.08633$, $w_2 = 0.395847$, $w_3 = 1.55$, $s = 0.065$ respectively, and the full-wave simulation results corresponding to these two exact parameter sets are shown in Fig. 11(b) and Fig. 11(c). The model output physical parameters corresponding the Specification 2 agree well with the exact physical parameters obtained by the full-wave simulation. For the Specification 3, the exact goal physical parameters beyond the range listed in Tab. 3 greatly, but the proposed model could provides a reliable initial point which is nearby the goal parameters.

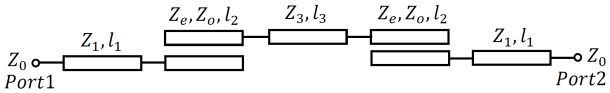


**Fig. 10.** The equivalent circuit structure corresponding to the second example.

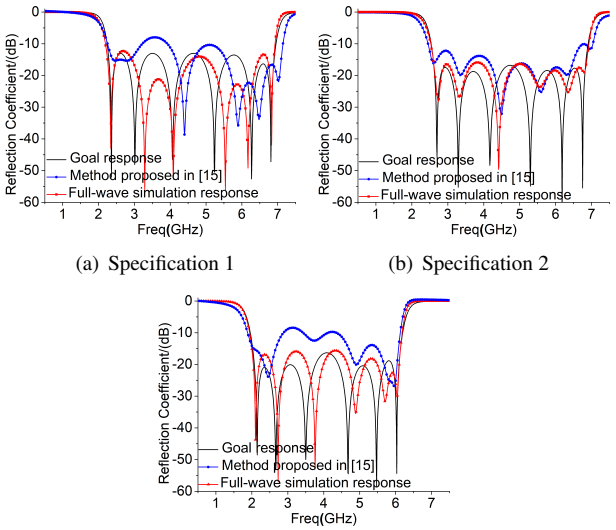


(a) Specification 1 (b) Specification 2

(c) Specification 3

**Fig. 11.** The goal magnitude responses and the full-wave simulation response corresponding to the specifications.

| Geometrical variables | | $l_1$ | $l_2$ | $l_3$ | $w_1$ | $w_2$ | $w_3$ | $s$ |
|---|---|---|---|---|---|---|---|---|
| Range | Min | 10.5 | 9 | 12.5 | 3 | 0.08 | 0.5 | 0.08 |
| | Max | 13 | 11 | 15 | 4.5 | 0.38 | 1.5 | 0.28 |

**Tab. 3.** Definition of training and testing data for the second example (unit:mm).

| Case | | 1 | 2 | 3 |
|---|---|---|---|---|
| Specification | $BW$ [GHz] | 2.09–7.10 | 2.36–7.05 | 1.76–6.35 |
| | $RL$ [dB] | –13 | –15 | –15 |
| EQC parameters | $Z_1$ [Ω] | 197.8 | 213.4 | 241.2 |
| | $Z_e$ [Ω] | 165.5 | 213.4 | 258.4 |
| | $Z_o$ [Ω] | 44.1 | 44.5 | 62.8 |
| | $Z_3$ [Ω] | 110.6 | 119.1 | 152.898 |
| | $l_1$ [mm] | 11.15 | 11.0 | 12.8 |
| | $l_2$ [mm] | 11.2 | 10.95 | 12.7 |
| | $l_3$ [mm] | 11.4 | 10.97 | 12.5 |

**Fig. 4.** The three goal magnitude response specifications and its corresponding equivalent circuit (EQC) parameters.

## 4. Conclusion

In this paper, a novel parametric modeling of microwave structure with customization responses by combining RBF neural network and Pole-Residue-Based transfer functions is proposed. For the design specification of microwave structure, our proposed model uses the insensitivity of the pole and residues to the geometrical variables and directly obtains the satisfying values of geometrical variables. The pole-resides vector is used as the input of the RBF network and the corresponding physical parameters values are used as the output of the network. The goal pole-residues corresponding to the

customization responses are obtained based on the the SA algorithm. After the training process of the RBF network, the goal pole-residues vector is inputted into the trained RBF network and the goal physical parameters is obtained directly. Two microwave structures in the cases of the narrower and wider sampling parameter ranges are used as the examples to prove the feasibility of the proposed model. The experimental verification results show that our proposed model provides a way to determine the target physical parameters quickly for the microwave structure with customization responses.

## References


[1] BRANDL, S., DYCZIJ-EDLINGER, R. Parametric model-order reduction for accelerating the gradient-based optimization of microwave structures using finite-elements. *IFAC-PapersOnLine*, 2018, vol. 51, no. 2, p. 190–195. DOI: 10.1016/j.ifacol.2018.03.033

[2] KOZIEL, S., OGURTSOV, S., LEIFSSON, L. Physics-based surrogates for low-cost modeling of microwave structures. *Procedia Computer Science*, 2013, vol. 18, p. 869–878. DOI: 10.1016/j.procs.2013.05.252

[3] ZHANG, Q., GUPTA, K., DEVABHAKTUNI, V. Artificial neural networks for RF and microwave design - From theory to practice. *IEEE Transactions on Microwave Theory and Techniques*, 2003, vol. 51, no. 4, p. 1339–1350. DOI: 10.1109/TMTT.2003.809179

[4] RAYAS-SANCHEZ, J. E. EM-based optimization of microwave circuits using artificial neural networks: The state-of-the-art. *IEEE Transactions on Microwave Theory and Techniques*, 2004, vol. 52, no. 1, p. 420–435. DOI: 10.1109/TMTT.2003.820897

[5] MKADEM, F., BOUMAIZA, S. Physically inspired neural network model for RF power amplifier behavioral modeling and digital predistortion. *IEEE Transactions on Microwave Theory and Techniques*, 2011, vol. 59, no. 4, p. 913–923. DOI: 10.1109/TMTT.2010.2098041

[6] ROOT, D. E. Future device modeling trends. *IEEE Microwave Magazine*, 2012, vol. 13, no. 7, p. 45–59. DOI: 10.1109/MMM.2012.2216095

[7] YU, H., CHALAMALASETTY, H., SWAMINATHAN, M. Modeling of voltage-controlled oscillators including I/O behavior using augmented neural networks. *IEEE Access*, 2019, vol. 7, p. 38973–38982. DOI: 10.1109/ACCESS.2019.2905136

[8] SADROSSADAT, A., CAO, Y., ZHANG, Q. Parametric modeling of microwave passive components using sensitivity-analysis-based adjoint neural-network technique. *IEEE Transactions on Microwave Theory and Techniques*, 2013, vol. 61, no. 1, p. 1733–1747. DOI: 10.1109/TMTT.2013.2253793

[9] SHARMA, K., PANDEY, G. Efficient modelling of compact microstrip antenna using machine learning. *AEU - International Journal of Electronics and Communications*, 2021, vol. 135, p. 1–13. DOI: 10.1016/j.aeue.2021.153739

[10] FENG, F., ZHANG, Q. Parametric modeling using sensitivity-based adjoint neuro-transfer functions for microwave passive components. In *IEEE MTT-S International Conference on Numerical Electromagnetic and Multiphysics Modeling and Optimization (NEMO)*. Ottawa (Canada), 2015, p. 1–3. DOI: 10.1109/NEMO.2015.7415028

[11] XIAO, L., SHAO, W., JIN, F. Multi-parameter modeling with ANN for antenna design. *IEEE Transactions on Antennas and Propagation*, 2016, vol. 66, no. 7, p. 3718–3723. DOI: 10.1109/TAP.2018.2823775

[12] FENG, F., ZHANG, C., MA, J. Parametric modeling of EM behavior of microwave components using combined neural networks and pole-residue-based transfer functions. *IEEE Transactions on Microwave Theory and Techniques*, 2016, vol. 64, no. 1, p. 60–77. DOI: 10.1109/TMTT.2015.2504099

[13] FENG, F., GONGAL-REDDY, V.-M.-R., ZHANG, C., et al. Parametric modeling of microwave components using adjoint neural networks and pole-residue transfer functions with EM sensitivity analysis. *IEEE Transactions on Microwave Theory and Techniques*, 2017, vol. 65, no. 6, p. 1955–1975. DOI: 10.1109/TMTT.2017.2650904

[14] ZHANG, J., FENG, F., ZHANG, W., et al. A novel training approach for parametric modeling of microwave passive components using Padé via Lanczos and EM sensitivities. *IEEE Transactions on Microwave Theory and Techniques*, 2020, vol. 68, no. 6, p. 2215–2233. DOI: 10.1109/TMTT.2020.2979445

[15] GUSTAVSEN, B., SEMLYEN, A. Rational approximation of frequency domain responses by vector fitting. *IEEE Transactions on Power Delivery*, 1999, vol. 14, no. 3, p. 1052–1061. DOI: 10.1109/61.772353


## About the Authors ...


**Yuhong MA** was born in 1996. He received his B.S. and M.S. degree in Electronic Science and Technology from the National University of Defense Technology in 2017 and 2019, respectively. He is currently working toward the Ph.D. degree in Electronic Science and Technology at the National University of Defense Technology. His research interests include microwave propagation and theory.

**Shuang WU** (corresponding author) was born in 1993. He received the B.S. degree in Electronic Engineering from Xidian University of China, Xian, China, in 2015, the M.S. degree in Electromagnetic Field and Microwave Technique from National University of Defense Technology, Changsha, China, in 2018. He is currently working toward the Ph.D. degree in Electronic Science and Technology at the National University of Defense Technology. His current research interests are machine learning.

**Ye YUAN** was born in 1994. He received his B.S. degree in Electronic Science and Technology from the Nanjing University of Aeronautics and Astronautics in 2016, the M.S. degree in Electromagnetic Field and Microwave Technique from National University of Defense Technology, Changsha, China, in 2019. He is currently working toward the Ph.D. degree in Electronic Science and Technology at the National University of Defense Technology. His current research interests are passive microwave circuits design and array signal processing.

**Naichang YUAN** was born in 1965. He received the M.S. and Ph.D. degrees in Electronic Science and Technology from the University Science and Technology of China in 1991 and 1994, respectively. He is currently a Professor with the College of Electronic Science and Engineering, National University of Defense Technology, Changsha, China. His research interests include microwave circuits design, wireless communication, and wave propagation.